

## Photophysics of resonantly and non-resonantly excited erbium doped Ge nanowires

This article has been downloaded from IOPscience. Please scroll down to see the full text article.

2012 Nanotechnology 23 065702

(<http://iopscience.iop.org/0957-4484/23/6/065702>)

View [the table of contents for this issue](#), or go to the [journal homepage](#) for more

Download details:

IP Address: 193.205.213.166

The article was downloaded on 18/01/2012 at 08:25

Please note that [terms and conditions apply](#).

# Photophysics of resonantly and non-resonantly excited erbium doped Ge nanowires

S Manna<sup>1</sup>, N Prtljaga<sup>2</sup>, S Das<sup>1</sup>, N Daldosso<sup>2</sup>, S K Ray<sup>1</sup> and L Pavesi<sup>2</sup>

<sup>1</sup> Department of Physics and Meteorology, Indian Institute of Technology Kharagpur, Kharagpur-721 302, India

<sup>2</sup> Dipartimento di Fisica, Laboratorio di Nanoscienze, Università di Trento, Via Sommarive 14, 38100 Povo (Trento), Italy

E-mail: [physkr@phy.iitkgp.ernet.in](mailto:physkr@phy.iitkgp.ernet.in)

Received 10 August 2011, in final form 12 December 2011

Published 17 January 2012

Online at [stacks.iop.org/Nano/23/065702](http://stacks.iop.org/Nano/23/065702)

## Abstract

We have fabricated Er doped germanium nanowires of different diameters by pulsed laser deposition and chemical methods. Er induced photoluminescence emission due to the intra-4f  $^4I_{13/2} \rightarrow ^4I_{15/2}$  transition of Er energy levels at 1.53  $\mu\text{m}$  has been achieved at room temperature using both resonant (980 nm) and non-resonant (325 nm) excitation of Er ions. The observed 1.53  $\mu\text{m}$  photoluminescence signal upon non-resonant 325 nm excitation is attributed to the Ge related oxygen deficiency centers surrounding the Ge core. For direct excitation, the infrared photoluminescence characteristics have been studied as a function of Er concentration, photon flux, and diameter of the nanowires. The Er related emission signal is found to be enhanced with increase in Er concentration, pump flux of 980 nm, and the nanowire diameter. The time resolved characteristics of the Er induced emission peak have been studied as a function of the pump flux as well as the diameter of the Ge nanowires.

(Some figures may appear in colour only in the online journal)

## 1. Introduction

Rare earth doped semiconductors have been shown to be remarkably important for the combination of electronic devices with optical elements [1]. During the last few decades, the optical properties of erbium doped semiconductor materials have been extensively studied due to the intra-4f  $^4I_{13/2} \rightarrow ^4I_{15/2}$  transition (first excited state to the ground state), which overlaps with the 1.53  $\mu\text{m}$  wavelength of maximum transmission of silica based optical fibers [2–4]. Er can be incorporated into nanostructures like quantum dots or nanocrystals (NCs) [5, 6], one-dimensional nanorods or nanowires [7], two-dimensional thin films [2] and also in bulk Si or Ge [8]. A lot of research has been carried out on low dimensional Si based systems [9–11]. In contrast, only a few papers discuss low dimensional Ge based systems. Since Ge has both a higher electron and hole mobility and a larger excitonic Bohr radius than Si and it is compatible with planar Si technology, efforts are being made to study the

optical properties of Er doped Ge nanostructures. Germanium possesses another two interesting properties:

- (i) the laser-pumping efficiency of Ge nanowires may be increased due to phonon confinement effects [12], i.e., the reduction of exciton–acoustic phonon interactions due to the host size reduction to the nanometer regime [13];
- (ii) the energy of the Ge exciton is close to the 1.54  $\mu\text{m}$   $^4I_{13/2} \rightarrow ^4I_{15/2}$  transition, which is also favorable for increase of the pump efficiency [14].

Moreover, the mechanism of non-resonant excitation of  $\text{Er}^{3+}$  ions due to an energy transfer process from the optically excited semiconductor nanocluster to the  $\text{Er}^{3+}$  ions is very appealing since it increases the effective Er excitation cross section. Although a lot of studies have been carried out using Er doped Ge nanocrystals [6, 15], not much attention has been paid to the use of one-dimensional Ge nanostructures. Wu *et al*

[16] has demonstrated the 1.53  $\mu\text{m}$  emission from Er doped Ge nanowires (NWs).

In this paper, we report the growth of Ge nanowires using a pulsed laser deposition (PLD) technique with *ex situ* doping of Er. We observed both visible emission as well as an infrared 1.53  $\mu\text{m}$  signal from the Er doped nanowires at room temperature. The characteristics of the Er induced PL emission using both resonant and non-resonant excitation are discussed.

## 2. Experimental details

Ge nanowires were grown on p-Si(100) substrates by a Au catalyst-assisted PLD technique [17] in a spherical chamber. Gold catalyst was deposited on the silicon substrates by thermal evaporation with thickness varying from 3 to 10 nm. Subsequently, the Au coated Si was annealed at 600 °C in  $\text{N}_2$  ambient, for the formation of Au nanoparticles. A pure Ge target was used as the source of Ge species using a KrF excimer laser ( $\lambda = 248 \text{ nm}$ ) for the ablation on the Au nanoparticle catalyzed Si, keeping the substrate vertically in front of the target. The laser energy density and the repetition rate were set to 2.3  $\text{J cm}^{-2}$  and 10 Hz, respectively. The deposition was carried out at a pressure of  $10^{-2}$  mbar for 1 h and the substrate temperature for growth was maintained at 600 °C. Prior to Ge deposition, the Au nanoparticle coated Si(100) substrate was pre-heated at the growth temperature for 5 min. In order to incorporate erbium onto the nanowire surface, nanowires of different average diameters ( $\sim 30$ ,  $\sim 80$ , and  $\sim 130 \text{ nm}$ ) were exposed to ethanolic solutions of  $\text{ErCl}_3 \cdot 6\text{H}_2\text{O}$  (by immersing) of different concentrations varying from 0.01 to 0.04 M and the samples were annealed thereafter from 600 to 800 °C in a 80%  $\text{N}_2 + 20\% \text{ O}_2$  atmosphere for 1 h using a drive-in diffusion process.

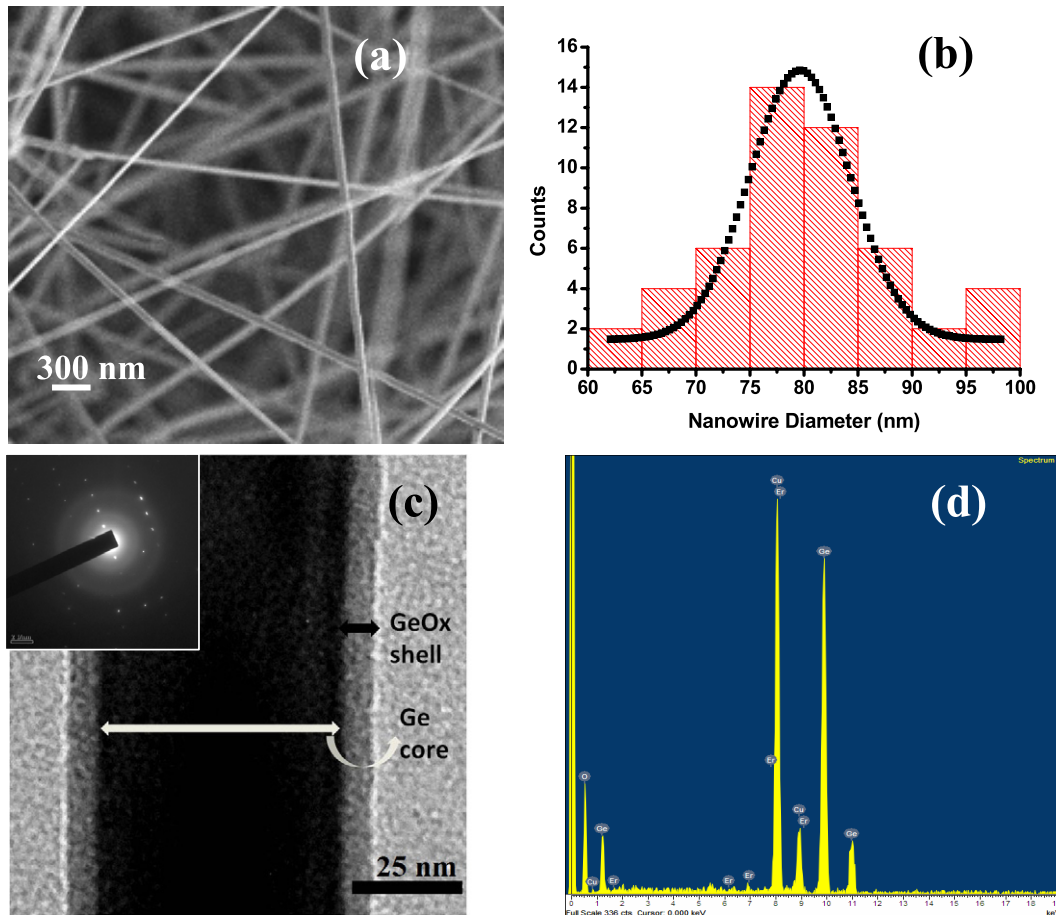
The nanowire morphology was characterized by field emission scanning electron microscopy (FESEM) and transmission electron microscopy (TEM). X-ray photoelectron spectroscopy (XPS) was used to probe the chemical bonding of the deposited films. Non-resonant PL measurements were carried out at room temperature using a He–Cd laser operating at 325 nm with an output power of 40 mW. The PL signals were analyzed using a TRIAX-320 monochromator and detected by a Hamamatsu R928 photomultiplier detector in the visible range and a liquid nitrogen cooled InGaAs detector in the IR region with a standard lock-in technique, where the laser beam was mechanically chopped at a frequency of 173 Hz. On the other hand, the resonant PL characteristics were studied at room temperature by exciting the erbium ions directly with a 980 nm diode laser having a spot area of 0.07  $\text{mm}^2$  and using a Chromex monochromator, and the signal was detected by a liquid nitrogen cooled InGaAs photomultiplier tube. All the spectra presented in this paper are corrected for the spectral response of the optical system. We also measured the lifetime of the 1.53  $\mu\text{m}$  emission peak using the 980 nm diode laser by external modulation of the laser diode drive current with a modulation frequency 10 Hz. The intrinsic response time of the measurement system was 2.3  $\mu\text{s}$ .

## 3. Results and discussion

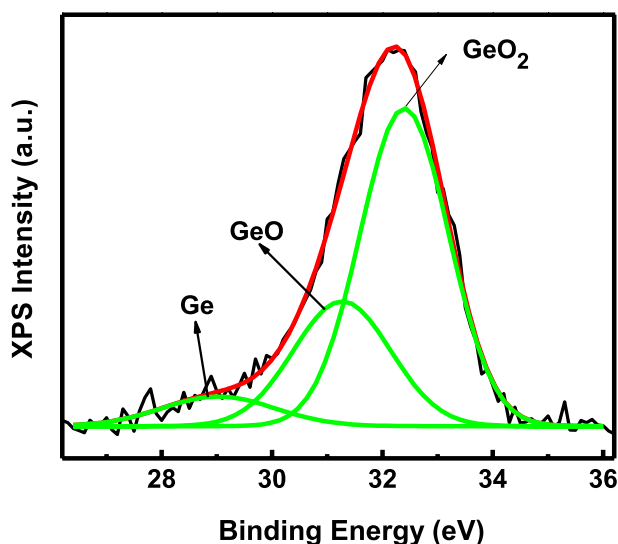
Three different sizes of nanowire (NW) with average diameters of 30, 80 and 130 nm were grown by varying the size of the Au nanoparticles coated on the Si wafer. Figure 1(a) shows a typical FESEM image of the Er doped Ge NWs with an average diameter of 80 nm. A bunch of interconnected Ge NWs is clearly observed. The size distribution is shown in figure 1(b). The size is found to vary from 60 to 100 nm with the peak of the distribution around 80 nm. Figure 1(c) shows a high-resolution TEM image of a wire with diameter  $\sim 73 \text{ nm}$ , which clearly reveals the formation of a core–shell structure. The selected area electron diffraction pattern (SAED) indicates that the dark region consists of a crystalline Ge core, surrounded by an amorphous layer of germanium sub-oxide ( $\text{GeO}_x$ ). The Ge core diameter is found to be  $\sim 56 \text{ nm}$  with a  $\text{GeO}_x$  shell thickness of  $\sim 8.5 \text{ nm}$ . The presence of  $\text{GeO}_x$  is also confirmed by the XPS analysis discussed in a later section. The Er contents of the Ge NWs doped using  $\text{ErCl}_3$  solutions of different molar concentrations were estimated from the energy dispersive analysis of x-ray (EDAX) system equipped with the TEM. We measured the average Er concentration in each single Er doped Ge NW of different doping level. Several nanowires of the same doping level were investigated in this TEM and EDAX analysis. For the used molar concentrations of 0.01 M, 0.025 M and 0.04 M of  $\text{ErCl}_3$ , the atomic concentrations of Er in the Ge nanowires were found to be  $\sim 0.8\%$ ,  $\sim 1.3\%$  and  $\sim 2.0\%$ , respectively. Figure 1(d) shows a typical EDAX spectrum of  $\sim 80 \text{ nm}$  nanowires doped with  $\sim 1.3 \text{ at.}\%$  Er. The characteristic x-ray signals of Ge, O and Er are observed from the nanowires.

Figure 2 shows the XPS spectrum of Ge 3d core-level electrons for a typical Ge nanowire sample with a diameter of 80 nm. The spectrum can be fitted by three components for germanium oxidation states. The first one is assigned to the metallic Ge ( $\text{Ge}^0$ ) around 29.0 eV and the other two peaks are attributed to the oxides of Ge. The binding energy peak shift of 2.2 eV with respect to elemental Ge is related to the  $\text{Ge}^{2+}$  oxidation state (GeO), whereas the other peak at 32.4 eV is assigned to Ge atoms in a  $\text{GeO}_2$ -like environment. Therefore, the XPS study indicates the presence of a GeODC ( $\text{GeO}_x$ ) shell surrounding the Ge nanowire core.

The photoluminescence of the Ge NWs at room temperature in the UV–visible range was studied using a 325 nm He–Cd laser as the exciting source. A broad PL peak in the visible wavelength around 400 nm is observed from the doped nanowires. Figure 3(a) typically shows the UV–visible PL emission spectrum with the peak position and shape remaining the same for all the sizes investigated here, and the room temperature infrared PL spectra of Er-incorporated Ge nanowires as a function of annealing temperature are shown in figure 3(b). Since the size of the nanowire is not low enough for significant quantum confinement, the PL peak ( $\sim 400 \text{ nm}$ ) does not originate from the quantum confinement of carriers. Since 325 nm is an indirect excitation source, the Er emission is attributed to the energy transfer from the Ge related oxygen deficiency centers (GeODCs),



**Figure 1.** (a) Field emission scanning electron microscopic image of Er doped Ge nanowires having a mean diameter of 80 nm. (b) Gaussian size distribution of the Ge nanowires shown in the micrograph (a). (c) High-resolution TEM image of a single Er doped Ge nanowire core embedded in a  $\text{GeO}_x$  sheath. Inset shows the SAED pattern of the nanowire. (d) Typical EDAX spectrum of the Er doped Ge nanowires shown in micrograph (a).



**Figure 2.** Ge 3d XPS spectrum of Ge nanowires with a mean diameter of 80 nm.

which are formed in the Ge core coating layer [18]. The oxygen deficiencies possess three energy states: the singlet state  $S_1$ , the triplet state  $T_1$ , and the ground state  $S_0$

[19, 20]. Due to the excitation by 325 nm (3.8 eV), GeODCs may be excited by direct absorption, which is followed by nonradiative relaxation by phonon emission to the lower levels of the triplet  $T_1$  state. From here the excited carriers may relax to the ground state  $S_0$  by a radiative decay of  $\sim 400$  nm (3.1 eV) emission. Since the  $T_1$  state consists of many levels, the emission is spectrally broad. This kind of emission is due to a HOMO (highest occupied molecular orbital)–LUMO (lowest occupied molecular orbital) transition, where both the HOMO and LUMO are located on the Ge atoms [19]. A competitive process is a nonradiative decay of the excited GeODCs to the ground state via an energy transfer to an  $\text{Er}^{3+}$  ion. In this way, the  $\text{Er}^{3+}$  ions will be excited from the ground  $^4I_{15/2}$  state to the excited  $^2H_{9/2}$  level, which is almost resonant with the  $T_1$  state. Then, the  $\text{Er}^{3+}$  ions de-excite to the  $^4I_{13/2}$  state by nonradiative relaxation from where a radiative transition to the ground state yields  $1.53 \mu\text{m}$  emission. This mechanism is shown schematically in figure 3(c). It may be noted that indirectly excited emission, as shown in figure 3(b), is quenched for annealing temperatures lower than  $600^\circ\text{C}$ . The  $\text{Er}^{3+}$  induced luminescence intensity increases with the annealing temperature from 600 to  $750^\circ\text{C}$ . The intensity is found to decrease with a further increase of the annealing temperature to  $800^\circ\text{C}$ . This observation indicates that under

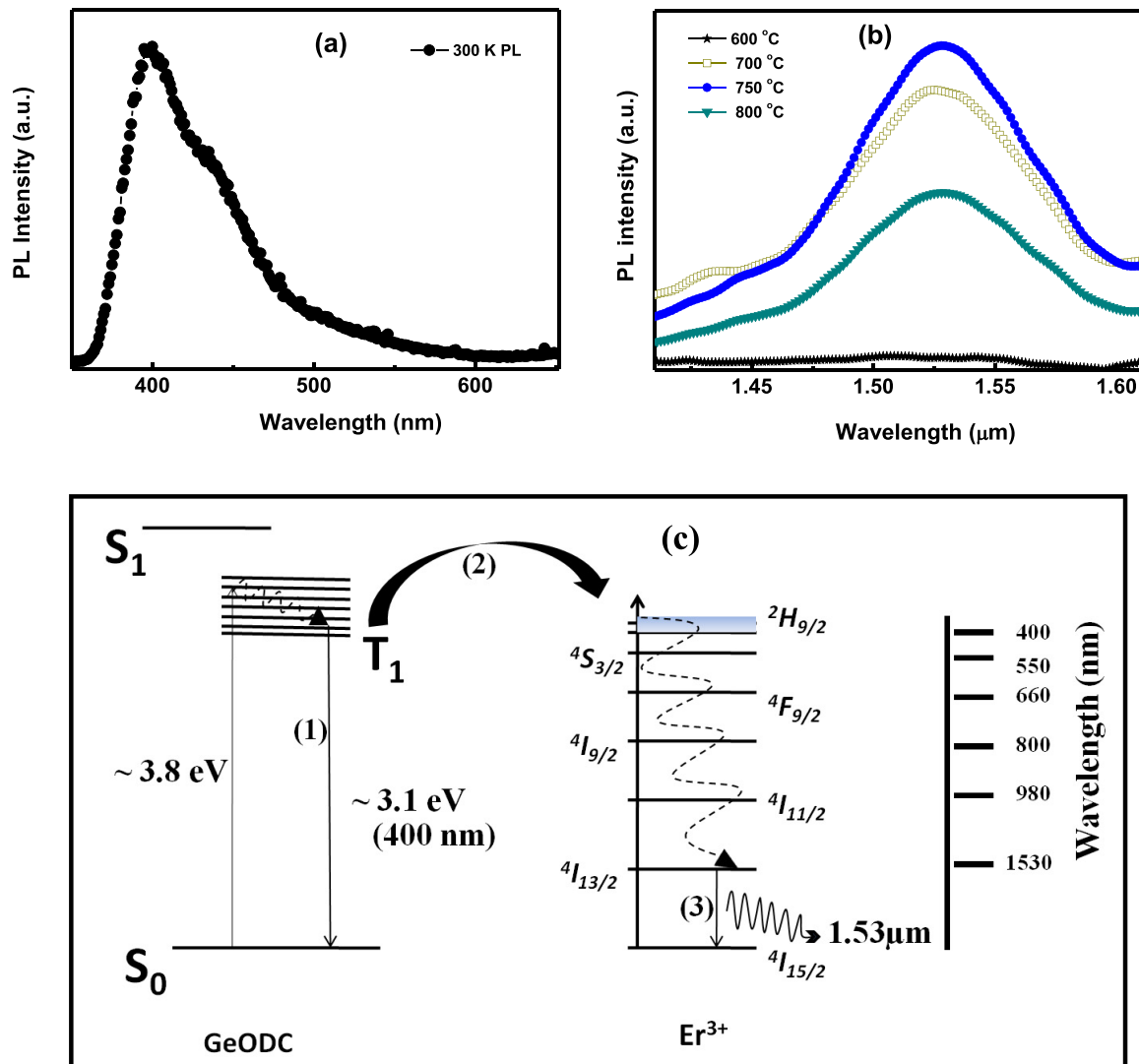


**Figure 3.** (a) UV–visible photoluminescence spectrum at room temperature for an 80 nm diameter Ge nanowire with ~1.3 at.% Er. (b) Infrared PL characteristics with different annealing temperatures. The excitation wavelength is 325 nm. (c) Energy transfer scheme from GeODCs to an Er<sup>3+</sup> ion: the radiative transition from the T<sub>1</sub> state is shown by (1); the downward arrow marked as (3) shows the 1.53 μm emission of Er<sup>3+</sup>; the wavy arrow from <sup>2</sup>H<sub>9/2</sub> to <sup>4</sup>I<sub>13/2</sub> indicates nonradiative transition, while energy transfer is denoted by (2).

non-resonant excitation, the Er<sup>3+</sup> ions are excited by the energy transfer from GeODCs, as discussed earlier. Basically, a minimum annealing temperature of 600 °C is necessary to form a local non-centrosymmetric coordination environment around the Er<sup>3+</sup> ions. These GeODCs are abundant until an annealing temperature of 750 °C, resulting in the strong enhancement of the Er<sup>3+</sup> related PL at 1.53 μm. With further increase in the annealing temperature in an O<sub>2</sub> ambient, stoichiometric GeO<sub>2</sub> is gradually formed from GeO<sub>x</sub>, leading to the depletion of GeODC defects. Therefore, the decrease in the number of GeODCs causes the reduction of Er<sup>3+</sup> PL above 750 °C. At these high temperatures, the indirect excitation process is almost diminished and thus Er<sup>3+</sup> can be excited only by direct resonant absorption processes, as was shown in stoichiometric GeO<sub>2</sub> [21]. It is interesting to note that the width of the Er emission peak depends on the excitation mechanism: pumping resonantly (980 nm) leads to a reduced line width of the central 1.53 μm emission peak compared to

non-resonant pumping. A possible explanation can be related to a site selection in the indirect Er excitation [2, 22].

If the wires contain Ge clusters or nanocrystals, they would act as sensitizers for Er excitation since visible PL emission is possible from the quantum mechanically confined carriers inside the Ge nanocrystals [23]. But the lack of such indirect excitation processes was confirmed by the absence of Er emission under non-resonant excitation at 632 nm. We then performed measurements by using the 980 nm excitation wavelength which is resonant with an internal transition (<sup>4</sup>I<sub>11/2</sub> to <sup>4</sup>I<sub>15/2</sub> state) of the Er<sup>3+</sup> ions. With this excitation condition no energy transfer from GeODCs to Er ions occurs. Figure 4(a) shows the 1.53 μm PL intensity variation with Er doping concentration for typical Ge NWs of 30 nm average diameter and annealed at 750 °C. It is observed that the PL intensity is enhanced with increasing doping concentration. It is possible that the increased doping of Ge nanowires lowers the symmetry of the Er<sup>3+</sup> ion/host structure leading

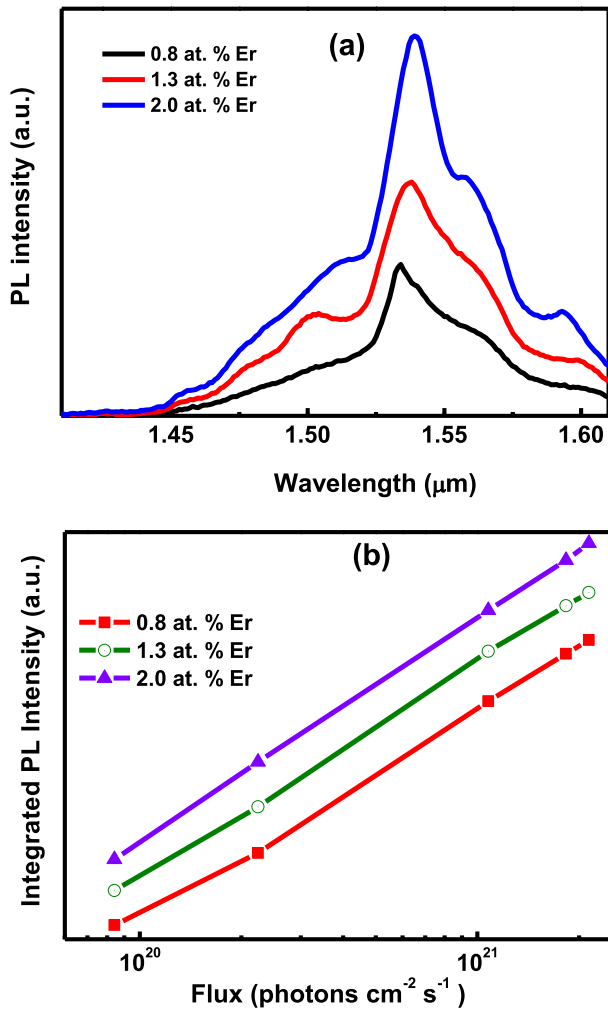


**Figure 4.** (a) Er induced PL emission characteristics of 30 nm diameter Ge nanowires with three different Er doping concentrations by 980 nm excitation wavelength. (b) log-log plot of the integrated 1.53  $\mu\text{m}$  PL emission intensity as a function of photon flux for different Er concentrations for 30 nm diameter Ge nanowires.

to an increase of the number of optically active  $\text{Er}^{3+}$  ions. Figure 4(b) shows the variation of the 1.53  $\mu\text{m}$  PL intensity with the laser flux for resonant excitation (980 nm). No saturation of the Er related emission occurs. This is in contrast with other observations for Er doped Si systems showing a sub-linear power dependence of the emission due either to the saturation of the optically active  $\text{Er}^{3+}$  ions [24] or to the localized Auger quenching [25]. Hence it emerges that the excitation phenomena of  $\text{Er}^{3+}$  ions in Ge NWs are different from those in Si.

We studied the time resolved photoluminescence characteristics of the Er emission peak excited by the 980 nm diode laser. The experimental decay curves and fitted results for 30 nm wide Ge NWs doped with 0.8 at.% Er for two different powers are shown in figure 5. The decay curves could be best fitted using a stretched exponential [26]

$$I_{\text{PL}}(t) = I_0 \exp(- (t/\tau)^\beta) \quad (1)$$

where  $\tau$  and  $\beta$  are the lifetime and dispersion parameter, respectively.

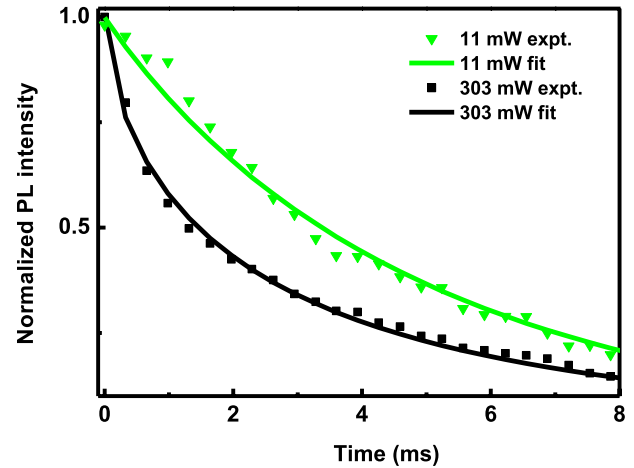


**Figure 5.** Photoluminescence decay characteristics of the 1.53  $\mu\text{m}$  Er emission peak by 980 nm excitation wavelength for excitation powers of 11 and 303 mW for 30 nm diameter 0.8 at.% Er doped Ge nanowires.

The mean lifetime  $\langle\tau\rangle$  can be calculated from the following relationship:

$$\langle\tau\rangle = \frac{\tau}{\beta} \Gamma\left(\frac{1}{\beta}\right) \quad (2)$$

where  $\Gamma$  denotes the Gamma function.

For example, the derived lifetimes are 5.03 ms and 3.65 ms, respectively, for excitation powers of 11 mW and 303 mW. It may be noticed that these lifetimes are as long as those for Er doped Si nanocrystals within a silica matrix [27]. The physical quantity that is measured in time resolved PL measurements is the total lifetime, which includes both radiative and nonradiative contributions. A change in either of the two different contributions leads to a change of the total PL lifetime. A decrease of the radiative lifetime would also provoke an increase of the emission/absorption cross sections. However, as the optical density of states is not likely to change under different pumping conditions all the changes could be associated with the variation of the nonradiative contribution to the total PL lifetime. Therefore, in our study, the reduction in lifetime at higher power can be explained by an up-conversion effect due to the interaction between two neighboring  $\text{Er}^{3+}$  ions both excited to the first excited state. In the interaction process, one de-excites to the ground state and the other is promoted to the  $^4\text{F}_{7/2}$  or  $^4\text{F}_{5/2}$  level. Now this excited ion will decay back to the first excited state or to the ground state; as a result, the first excited state population will be depleted by one or two ions, respectively. This up-conversion interaction depends strongly on the concentration of excited  $\text{Er}^{3+}$  ions. Other mechanisms which might have effects on the lifetime are the nonradiative recombination processes such as the excited state absorption (an excited  $\text{Er}^{3+}$  ion absorbs a pump photon and goes to the higher excited state) and also the nonradiative decay rate increase attributed to the defects in the oxide matrix.

The decay times of the nanowires with three different diameters as a function of the 980 nm pump flux are presented in figure 6. A decrease of PL decay time with flux is observed

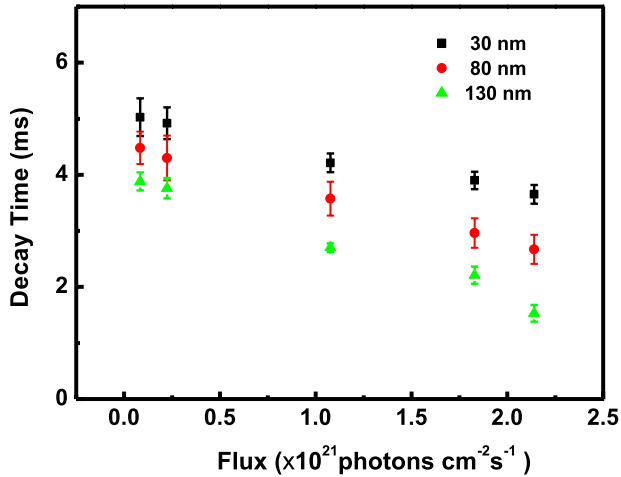


**Figure 6.** Decay time variations with 980 nm pump flux for nanowires of different diameters.

for nanowires having different diameters. Now for the same pump flux, the decay time decreases with increase in diameter of the nanowire. So this effect could be attributed to the complex morphology and curvature of the nanowires having an impact on the PL decay time. To explain the above, one may consider the spontaneous transition rate  $W(R)$  of a dipole from Fermi's golden rule:

$$W(R) = \frac{\pi\omega}{\hbar\varepsilon(R)} |M_{fi}|^2 \rho(\omega, R) \quad (3)$$

where  $M_{fi}$  is the dipole transition matrix element of the  ${}^4I_{13/2} \rightarrow {}^4I_{15/2}$  electronic transition,  $\omega$  is the angular frequency of the radiation,  $\rho$  is the polarization- and angle-averaged local optical density of states [28] at a distance  $z$  from the interface and  $\varepsilon(R)$  is the position-dependent dielectric function. A stronger confinement of the  $\text{Er}^{3+}$  ions within the oxidized shell of a Ge NW is likely to reduce the optical density of states for emission and the resultant transition rate  $W(R)$ . This leads to increase of the luminescence lifetime ( $\tau$ ), which has been experimentally observed and presented in figure 6. For a particular photon flux, the lifetime decreases with increase in the size of the nanowires. Typically, for nanowires of mean diameter 30 nm, the lifetime varies from 5.03 to 3.65 ms with an increase of power from 11 to 303 mW. For the 80 and 130 nm diameters, the lifetimes vary from 4.48 to 2.67 ms and 3.88 to 1.53 ms, respectively, for the same variation of power. This indicates that with increase in diameter, the degree of confinement of  $\text{Er}^{3+}$  ions is reduced. It is proposed that the nanowires could act like waveguides and in doing so limit the number of emission modes available, leading to a decrease of the optical DOS and a drop in the transition rate with increased confinement. This is in agreement with previously reported results on Er doped silica NWs [29].

The diameter dependent infrared PL spectra with a 980 nm pump with  $\sim 0.8$  at.% Er doping are presented in figure 7. It is observed that with the increase in diameter, the photoluminescence intensity increases substantially for constant doping concentration. Although the PL decay time

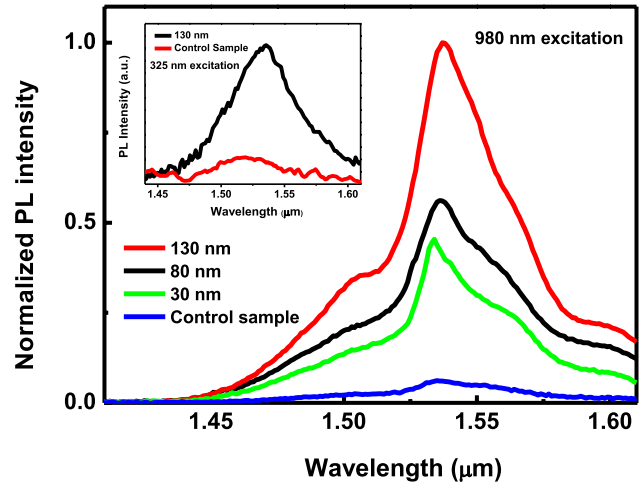


**Figure 7.** Diameter dependent Er induced PL emission characteristics of Ge nanowires with the same Er doping concentration ( $\sim 0.8$  at.%) by 980 nm excitation wavelength. The inset shows the infrared PL emission of Er doped wires of 130 nm average diameter under a 325 nm pump in comparison to the control sample.

is less for wider NWs due to the reduction of the local optical DOS of the  $\text{Er}^{3+}$  ions, the Er induced PL intensity increases with nanowire diameter. The enhanced PL intensity for larger diameter is due to the large number of optically active  $\text{Er}^{3+}$  ions for 130 nm diameter NW compared to 30 nm wide NW. It is important to note that usually the gold-catalyzed growth of nanowires through a vapor-liquid-solid mechanism also involves the simultaneous growth of a two-dimensional film on the substrate regions not covered by the metal catalyst. This film might also contribute to the Er induced PL emission. As a consequence, the optical emission of the system could be the sum of two different contributions, one coming from the NWs, the other from this planar layer. This is why the control sample of Er doped Ge was grown without any gold nanoparticle catalysts. From figure 7, it is clear that the Er PL signal is coming mostly from the Ge nanowires, being much higher than the planar Er doped Ge layer. The inset of figure 7 indicates that upon 325 nm indirect excitation, the acquired  $1.53 \mu\text{m}$  PL intensity is more for the 130 nm mean diameter nanowires than for the control sample without nanowires, revealing the increased efficiency of Er excitation for the Ge nanowire sample.

#### 4. Conclusions

In conclusion, we have grown Ge nanowires by pulsed laser deposition. The fabricated nanowires have been doped by Er using a chemical method. Defect induced photoluminescence emission due to GeODCs is observed at room temperature from the Ge nanowires. This PL emission leads to a carrier mediated pathway for Er excitation under non-resonant excitation (325 nm) for  $\text{Er}^{3+}$  ions. For resonant excitation with 980 nm, the intensity of Er induced luminescence increases with increase of Er concentration from 0.8 to 2 at.%. This is attributed to the achievement of an increase of optically

active Er<sup>3+</sup> ions for a given nanowire diameter. This is also corroborated by the flux dependent PL intensity variation for different Er concentrations. The average lifetime of the Er PL line at 1.53  $\mu\text{m}$  Er emission decreases with an increase in the resonant 980 nm pump flux for each nanowire. On the other hand, a reduction of the PL lifetime takes place with an increase in diameter; this is considered to originate from the reduction of the local optical DOS of Er<sup>3+</sup> ions for stronger confinement in the small NWs, as compared to the larger ones. The diameter dependent PL spectra show a higher PL intensity from larger NWs in spite of the lower decay time, because of the higher density of optically active Er ions.

## Acknowledgments

The work is supported by the ITPAR-DST Nanophotonics program between the University of Trento, Italy and IIT Kharagpur, India. The authors thank Dr S Maikap for XPS measurements.

## References

- [1] Kenyon A J 2002 *Prog. Quantum Electron.* **26** 225
- [2] Polman A 1997 *J. Appl. Phys.* **82** 1
- [3] Kimerling L C 2000 *Appl. Surf. Sci.* **159** 8
- [4] John J S, Coffey J L, Chen Y D and Pinizzotto R F 1999 *J. Am. Chem. Soc.* **121** 1888
- [5] Kenyon A J 2005 *Semicond. Sci. Technol.* **20** R65
- [6] Kanjilal A, Rebohle L, Baddela N K, Zhou S, Voelskow M, Skorupa W and Helm M 2009 *Phys. Rev. B* **79** 161302
- [7] Huang C T, Hsin C L, Huang K W, Lee C Y, Yeh P H, Chen U S and Chen L J 2007 *Appl. Phys. Lett.* **91** 093133
- [8] Coffa S, Franzo G, Priolo F, Polman A and Serna R 1994 *Phys. Rev. B* **49** 16313
- [9] Garrido B, García C, Seo S Y, Pellegrino P, Navarro-Urrios D, Daldosso N, Pavesi L, Gourbilleau F and Rizk R 2007 *Phys. Rev. B* **76** 245308
- [10] Polman A and Veggel F V 2004 *J. Opt. Soc. Am. B* **21** 871
- [11] Van den Hoven G N, Shin J H, Polman A, Lombardo S and Campisano S U 1995 *J. Appl. Phys.* **78** 2642
- [12] Zhang Y F, Tang Y H, Wang N, Lee C S, Bello I and Lee S T 2000 *Phys. Rev. B* **61** 4518
- [13] Zhao H, Wachter S and Kalt H 2002 *Phys. Rev. B* **66** 085337
- [14] Chen J H, Pang D, Cheong H M, Wickboldt P and Paul W 1996 *Appl. Phys. Lett.* **67** 2182
- [15] Kanjilal A, Rebohle L, Voelskow M, Skorupa W and Helm M 2009 *Appl. Phys. Lett.* **94** 51903
- [16] Wu J, Panchaipetch P, Wallace R M and Coffey J L 2004 *Adv. Mater.* **16** 1444
- [17] Morales A M and Lieber C M 1998 *Science* **279** 208
- [18] Kanjilal A, Rebohle L, Voelskow M, Skorupa W and Helm M 2009 *J. Appl. Phys.* **106** 26104
- [19] Kanjilal A, Tsushima S, Götz C, Rebohle L, Voelskow M, Skorupa W and Helm M 2009 *J. Appl. Phys.* **106** 63112
- [20] Ginzburg L P, Gordeev A A, Gorchakov A P and Jilinsky A P 1995 *J. Non-Cryst. Solids* **183** 234
- [21] Wu J and Coffey J L 2007 *Chem. Mater.* **19** 6266
- [22] Polman A, Jacobson D C, Eaglesham D J, Kistler R C and Poate J M 1991 *J. Appl. Phys.* **70** 3778
- [23] Das S, Das K, Singha R K, Dhar A and Ray S K 2007 *Appl. Phys. Lett.* **91** 233118
- [24] Coffa S, Priolo F, Franzo G, Bellani V, Carnera A and Spinella C 1993 *Phys. Rev. B* **48** 11782
- [25] Benton J L, Eaglesham D J, Almonte M, Citrin P H, Marcus M A, Adler D L, Jacobsen D C and Poate J M 1993 *Mater. Res. Soc. Symp. Proc.* **301** 181
- [26] Pavesi L and Ceschini M 1993 *Phys. Rev. B* **48** 17625
- [27] Chryssou C E, Kenyon A J, Iwayama T S, Pitt C W and Hole D E 1999 *Appl. Phys. Lett.* **75** 2011
- [28] De Dood M J A, Slooff L H, Polman A, Moroz A and Blaaderen A V 2001 *Phys. Rev. A* **64** 033807
- [29] Elliman R G, Wilkinson A R, Kim T-H, Sekhar P K and Bhansali S 2008 *J. Appl. Phys.* **103** 104304